Polymer Journal, Vol. 7, No. 4, pp 467—480 (1975)

Rheo-Optical Studies of Drawn Polyethylene Films

Shigeharu ONOGI, Akira TANAKA, Yoshiaki ISHIKAWA, and Toshio IGARASHI

Department of Polymer Chemistry, Kyoto University, Kyoto 606, Japan.

(Received December 16, 1974)

ABSTRACT: Previous studies of the rheo-optical properties of polyolefins have shown that the rheo-optical properties of undrawn polyolefins can be well explained by considering three deformation mechanisms. When spherulites in polyolefins are broken either partially or completely, drastic changes in the crystalline structure, and hence in the rheo-optical properties, should occur. In order to make this point clear experimentally, birefringence relaxation and stress relaxation were measured simultaneously for low density polyethylene films drawn to various extents.

For undrawn and weakly drawn films, the strain—optical coefficient increased with increasing time, while for a highly drawn film, it decreased with increasing time. This indicates that the highly drawn films do not exhibit the mechanism of crystalline orientation, which causes the birefringence to increase with time.

The time curves for the strain-optical coefficient and the relaxation modulus obtained at various temperatures could be superposed by vertical and horizontal shifts. Then, from the horizontal shift factors, activation energies for the rheo-optical and viscoelastic relaxation processes were determined. The activation energies for the highly drawn films are much higher than those for the undrawn and weakly drawn films, suggesting the existence of a fourth deformation mechanism.

Relaxation experiments were also carried out for undrawn low density polyethylene at different strain levels ranging from 3% to 12%. The effect of strain level appears to be equivalent to the effect of drawing in the sense that the peak of the relaxation spectrum at the shorter relaxation times decreases with increasing strain.

KEY WORDS Rheo-Optics / Birefringence / Viscoelasticity / Drawing / Polyethylene /

The rheo-optical properties of polyethylene and polypropylene have been studied in some detail over the past decade.[1] These studies have shown that the rheo-optical and viscoelastic properties of undrawn polyolefins can be well explained by considering three deformation mechanisms: the deformation of the spherulites as a whole, the orientation of crystals in the spherulites, and the orientation of amorphous molecular chains. These mechanisms were proposed by us in a paper published in 1964.[2] Among the three mechanisms, crystalline orientation produces certain birefringence effects (for example, in the case of polyethylene, an increase in birefringence with time during stress relaxation or a decrease in dynamic birefringence with frequency) which seem to be peculiar to the polyolefins. Such an increase in birefringence with time was not observed at all in the case of nylon 11 and nylon 12, as was described in a previous paper.[3]

When spherulites in polyolefins are broken either partially or completely, as, for example, during drawing, drastic changes in the crystalline structure, and hence in the rheo-optical properties, should occur. In order to make this point clear experimentally, stress relaxation and birefringence relaxation were measured for low density polyethylene over wide ranges of time and temperature and at various draw ratios.

Relaxation experiments were also carried out for undrawn films of polyethylene, at different strain levels ranging from 3% to 12%, to compare the effect of drawing with that of strain level.

EXPERIMENTS

Materials

As mentioned above, low density polyethylene films drawn to various extents were used in this study. To prepare the films, pellets of low density polyethylene B-128, produced by Ube Industries, Ltd., were employed. The number-average molecular weight of this material is about 27,000, and the degree of branching is 2.7/100 carbon atoms.

First, pellets of this material were placed between two aluminum plates and pressed for several minutes in a laboratory press at 160°C and a pressure of 30 kg/cm^2. After being released from the pressure, the melt was pressed again under the same conditions. After 5 min, the sample, which was still contained between the aluminum plates, was plunged into an ice—water bath.

Long strips were cut from the quenched films thus obtained, and the strips were drawn with a hand stretcher in a water bath at 60° or 100°C, depending on the draw ratio desired. The drawn films were further heat-treated in an oven at 105°C for 45 min and then subjected to certain measurements. Pitch lines were marked on the films and the separation of these lines was measured to determine the draw ratio; caution was taken to use a uniformly drawn portion of the film for the measurements.

The sample codes, draw ratios, drawing temperatures, and temperatures of heat-treatment (or thermal setting) are listed in Table I. In this table, A is the undrawn film, B to E are the films which were drawn uniformly before necking occurred, and F to H are films highly drawn after necking occurred.

Table I. The sample codes, draw ratios, drawing temperatures, and temperatures of heat-treatment for the samples employed

Sample	Draw ratio	Drawing temp, °C	Temperatures of heat-treatment, °C
A	1.00	—	—
B	1.30	60	105
C	1.55	60	105
D	1.80	60	105
E	2.00	100	105
F	3.20	100	105
G	4.00	60	105
H	5.00	100	105

For relaxation measurements at different strain levels, a different type of low density polyethylene, Dow 544, was used. To prepare the films, pellets were melt-pressed for 15 min at 140°C at 25 kg/cm^2 in the laboratory press used previously; the samples were then cooled gradually in the press to room temperature. The films thus obtained were further heat-treated for 5 min in boiling water and then gradually cooled in water to room temperature.

Measurements

The density of the films was measured by the floatation method using an ethanol—water system at 30°C.

The stress relaxation and birefringence relaxation measurements were made on the same instrument as was used previously.[4] It consists of an Instron-type tensile tester (Tensilon UTM-IV) combined with an optical system for measuring the birefringence continuously by an intensity method.

X-ray diffraction measurements were also carried out on a diffractometer (Model VD-1) manufactured by Shimadzu Manufacturing Co., which was described earlier.[5]

RESULTS AND DISCUSSION

Characterization of the Drawn Films

The density of the various samples is plotted against draw ratio in Figure 1. Also plotted is the degree of crystallinity X_c, which was evaluated

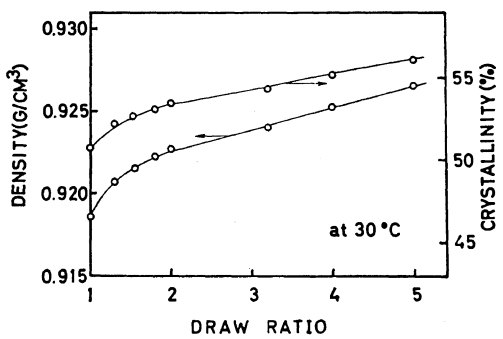

Figure 1. Density and degree of crystallinity plotted against draw ratio for all the samples at 30°C.

from the density by using the following equation:

$$X_c=\frac{v-v_a}{v_c-v_a}\times 100(\%) \qquad (1)$$

where v is the specific volume of the film, and v_a and v_c are, respectively, the specific volumes for the amorphous and crystalline phases. The quantities v_a and v_c were evaluated from the following equations proposed by Chiang and Flory:[6]

$$v_a=1.152+8.8\times 10^{-4}T \qquad (2)$$

and

$$v_c=0.993+3.0\times 10^{-4}T \qquad (3)$$

where T is the temperature in °C. As is evident from Figure 1, the density and degree of crystallinity first increase rapidly and then more gradually with increasing draw ratio.

The orientation functions F_a, F_b, F_c for the *a*-, *b*-, and *c*-crystal axes were evaluated from the dependence of the X-ray diffraction intensities for the (110) and (200) planes on the azimuthal angle. The results are shown as a function of draw ratio in Figure 2. For sample B, which

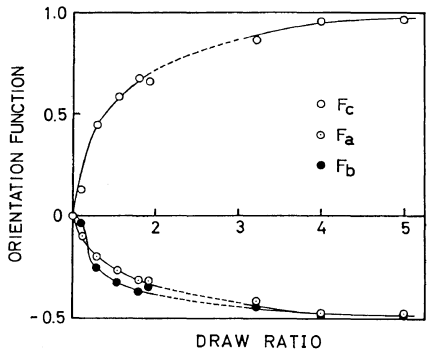

Figure 2. Orientation functions F_a, F_b, and F_c plotted against draw ratio.

has a draw ratio of 1.1, the negative value of F_a is larger than F_b, but for samples of higher draw ratios, F_b is larger than F_a. In samples G and H, those having the highest draw ratios, the *c*-axis orients almost completely to the drawing direction, while the *a*- and *b*-axes orient perpendicular to the drawing direction. Undoubtedly, these samples have fiber structure. The portion of the curve drawn with a broken line in the figure is the range where film strips showed necking during drawing; these film samples were neither uniform enough nor long enough to be used for the relaxation measurements.

The birefringence of all the sample films was measured by means of a polarizing microscope equipped with a Babinet compensator. The total birefringence Δ for polyethylene can be expressed by

$$\Delta=X_c\Delta_c+(1-X_c)\Delta_a+\Delta_f \qquad (4)$$

where X_c is the degree of crystallinity in the volume fraction and Δ_f is the form birefringence.[7] Δ_c in this equation is given by

$$\Delta_c=F_a(n_a-n_c)+F_b(n_b-n_c) \qquad (5)$$

where n_a, n_b, and n_c are the principal refractive indexes for the *a*-, *b*-, and *c*-axes. Using the values $n_a=1.514$, $n_b=1.519$, and $n_c=1.575$, as determined elsewhere for *n*-paraffins,[8] and the values for the orientation functions and the degree of crystallinity obtained above, we can evaluate the contribution of the crystalline phase, $X_c\Delta_c$. Then, ignoring Δ_f, the contribution from the amorphous phase, $(1-X_c)\Delta_a$ can be determined as the difference between Δ and Δ_c. The total birefringence and the contributions from the crystalline and amorphous phases thus evaluated are plotted against draw ratio in Figure 3. The tendencies of the curves in this figure are very similar to those reported by Hoshino, *et al.*[9], indicating that the drawn films employed here are not special ones.

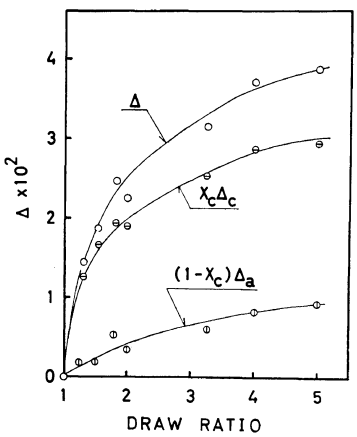

Figure 3. Total birefringence and the contributions from the crystalline and amorphous phases plotted against draw ratio.

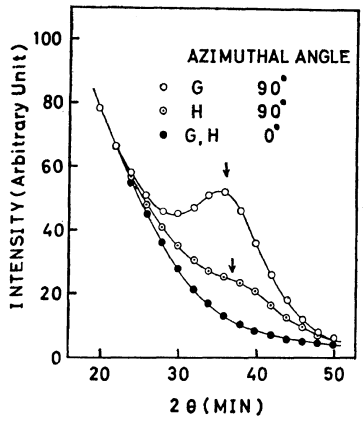

Figure 4. Small angle X-ray scattering intensities at azimuthal angles of 90° and 0° plotted against 2θ for the highly drawn samples G and H.

In Figure 4 are given the small-angle X-ray scattering intensity curves obtained for the samples G and H. The X-ray beam was applied perpendicular to the film plane. As is evident from this figure, the two curves for G and H at an azimuthal angle of 90° show a peak at around $2\theta=35'$. The long period evaluated from the Bragg condition was 148 Å for G, and 144 Å for H. The peak appears at a constant Bragg angle, independent of azimuthal angle, but its intensity decreases with decreasing azimuthal angle. At azimuthal angles smaller than 30°, no distinct peak is observed. These results are consistent with the fact that the samples G and H have fiber structure. Sample H shows a peak lower and broader than that of sample G, despite its higher draw ratio. This is probably due to the fact that H was drawn at a lower temperature, and hence its stratiform structure is less uniform.

The other samples A to F do not show any distinct peak in their small angle scattering intensity curves.

The stress—strain curves and the birefringence—strain curves obtained for all the samples are given in Figures 5a and b. The film (5 cm × 1.5 cm × 250 μ) was elongated at a constant speed of 10%/min, and the strain was defined as (elongation)/(initial length) × (draw ratio) in order to make clear the variation from the undrawn state. Only the highly drawn samples F, G, and H give almost linear stress—strain curves over the strain range covered by this study. On the other hand, the birefringence—strain curves for all the samples are almost linear. The birefringence at a given strain and the variation of birefringence with strain also decrease with increasing draw ratio. Furthermore, the birefringence—strain curves appear to be classified into three groups, depending on the magnitudes

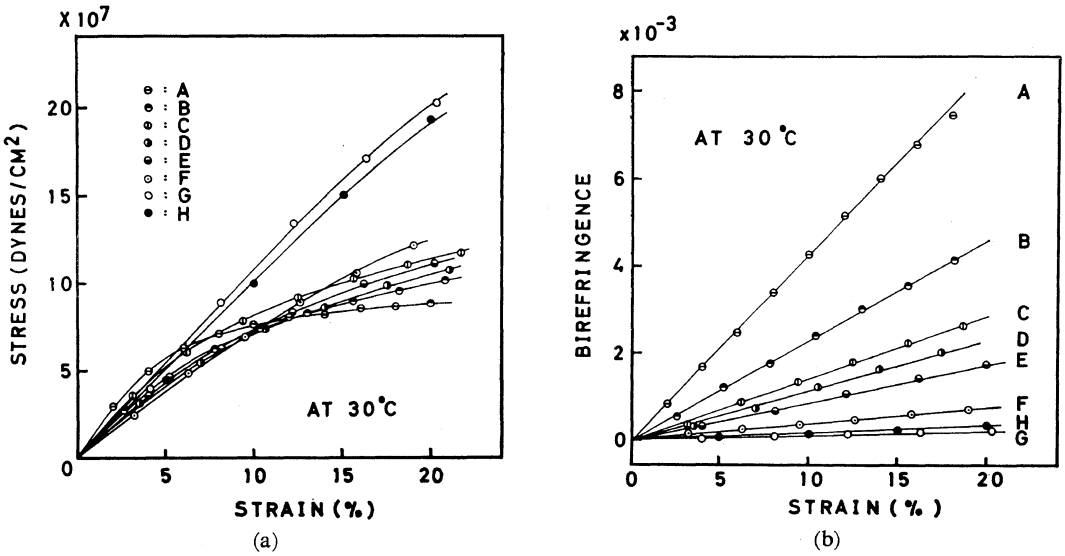

Figure 5. Stress—strain curves (a) and birefringence—strain curves (b) for all the samples.

of the birefringence and the draw ratio. The three groups would seem to be the curve for A, the curves for B to E, and the curves for F to H.

Stress Relaxation and Birefringence Relaxation

Several strips, 5 cm in length and 1.3—1.5 cm

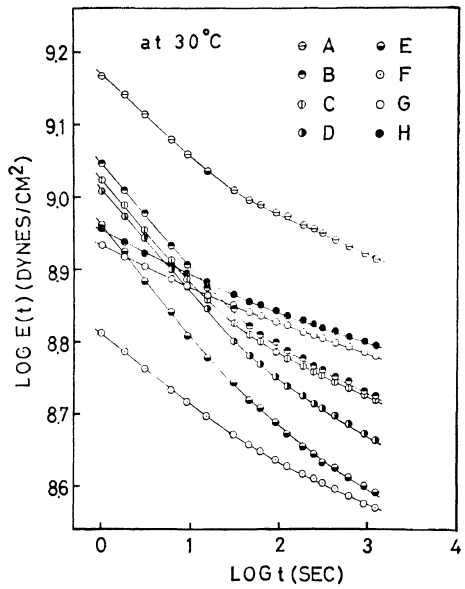

Figure 6. Relaxation modulus logarithmically plotted against time for all the samples at 30°C.

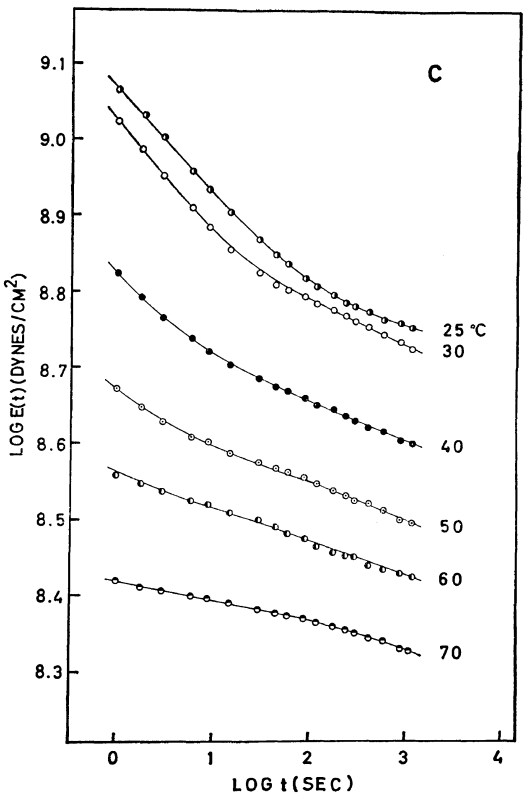

Figure 8. Relaxation modulus measured at various temperatures for sample C.

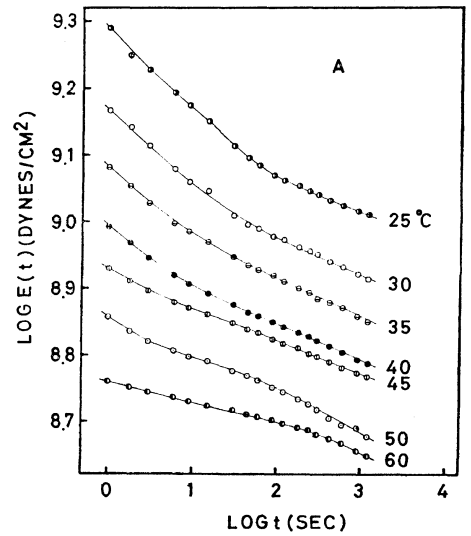

Figure 7. Relaxation modulus measured at various temperatures for sample A.

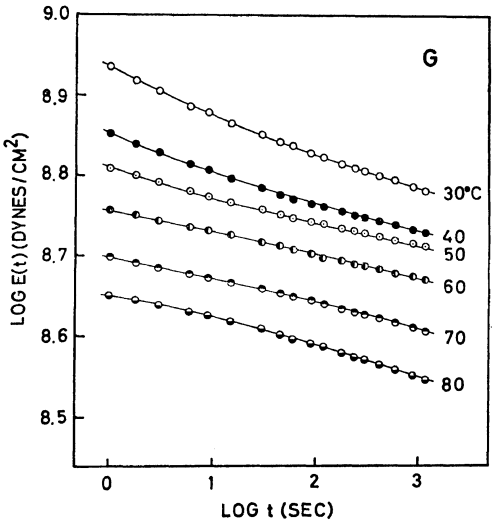

Figure 9. Relaxation modulus measured at various temperatures for sample G.

in width, were cut from the samples A to H and used for relaxation measurements. The strip was first elongated at a constant speed of 20 cm/min to various extents (about 3% for samples A to E and about 8% for samples F to H); then the stress relaxation and birefringence relaxation were measured at constant length. Here again, the strain γ is defined as (elongation)/(initial length)$\times$(draw ratio).

The results of stress relaxation for the samples A to H at 30°C are shown in Figure 6. As is evident from this figure, the relaxation modulus $E(t)$(=stress/strain) for all the samples decreases with increasing time, but the tendency is different from sample to sample. Therefore, further measurements at various temperatures ranging from 25° to 80°C were carried out on the four samples A, C, G, and H. The results are given in Figures 7 to 10.

The birefringence relaxation data corresponding to the stress relaxation data shown in Figure 6 is given in Figure 11. In the case of the undrawn sample A and the weakly drawn samples B to E, the strain—optical coefficients Δ/γ increases with time at all temperatures involved. In marked contrast to this, the strain-optical coefficient for the highly drawn films G and H decreases with increasing time. In the case of the intermediate sample F, the strain-optical coefficient is almost constant, independent of time.

In order to establish the temperature dependence of the birefringence more precisely, the birefringence relaxation for the samples A, C, G, and H was also measured at various temperatures ranging from 25° to 80°C. The results are shown in Figures 12 to 15. It is clear from these figures that the strain-optical coefficient for samples A and C always increases with time until it reaches a limiting value, which value depends on temperature. On the other hand, the strain-optical coefficients for the samples G and H decrease continuously with increasing time, showing no limiting values in the time range covered by this study.

In order to make the temperature dependence of the strain-optical coefficient clear, its value at 1000 sec is plotted against temperature in Figure 16. The plot shows a peak. The temperature at which this peak appears, T_{max}, is about 40°C for the undrawn film A, but it increases

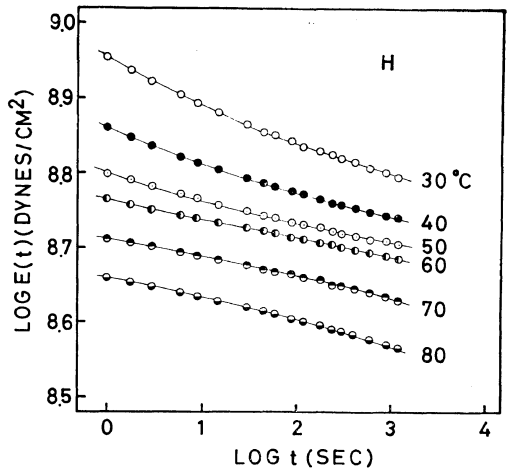

Figure 10. Relaxation modulus measured at various temperatures for sample H.

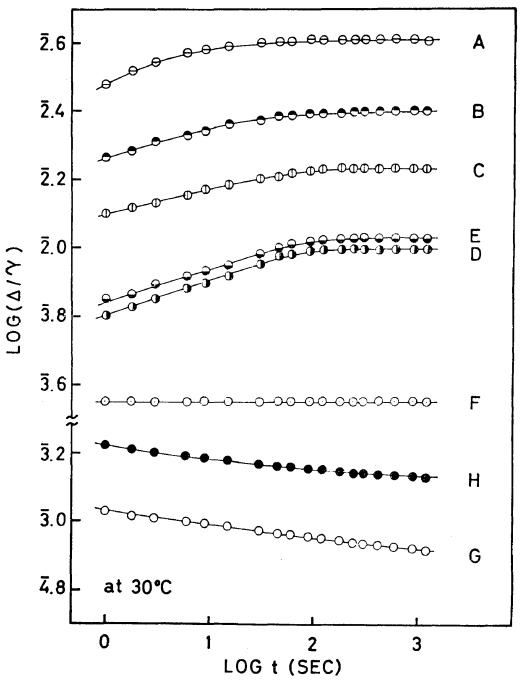

Figure 11. Strain—optical coefficient logarithmically plotted against time for all the samples at 30°C.

with increasing draw ratio to about 60°C for sample G and about 70°C for sample H. This result is consistent with our previous finding that T_{max} increases with increasing crystallinity.[5,10]

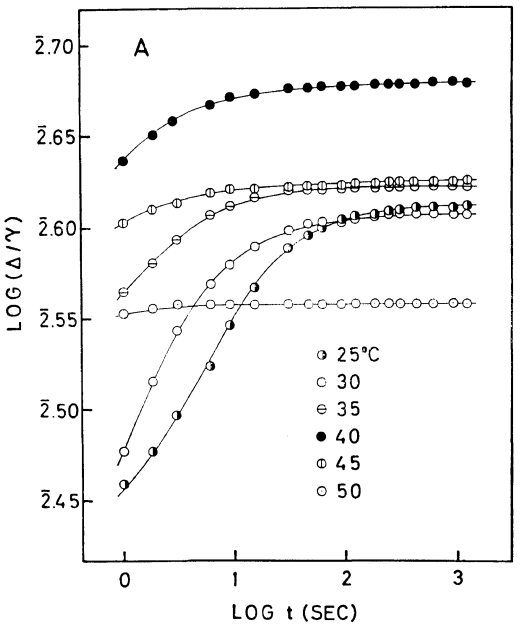

Figure 12. Strain—optical coefficient measured at various temperatures for sample A.

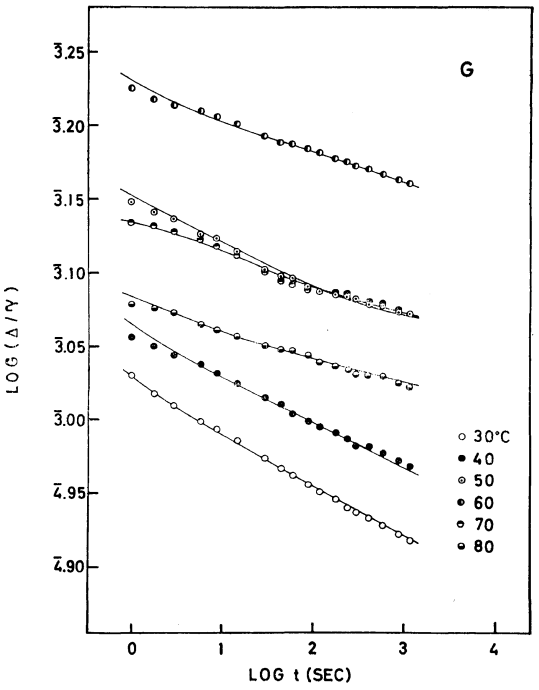

Figure 14. Strain—optical coefficient measured at various temperatures for sample G.

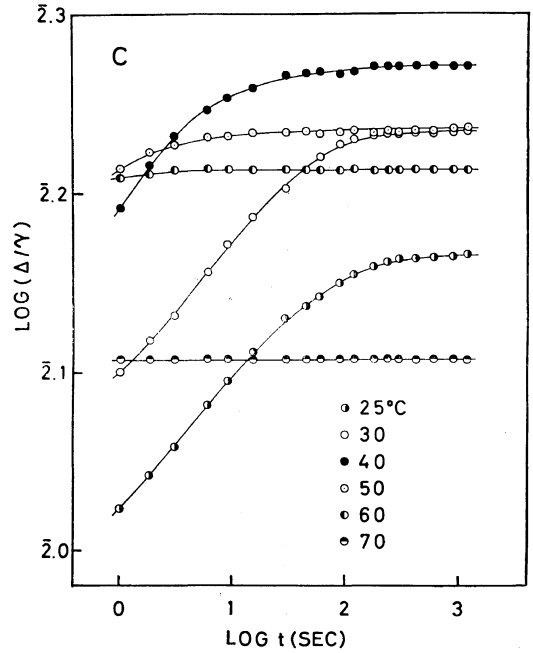

Figure 13. Strain—optical coefficient measured at various temperatures for sample C.

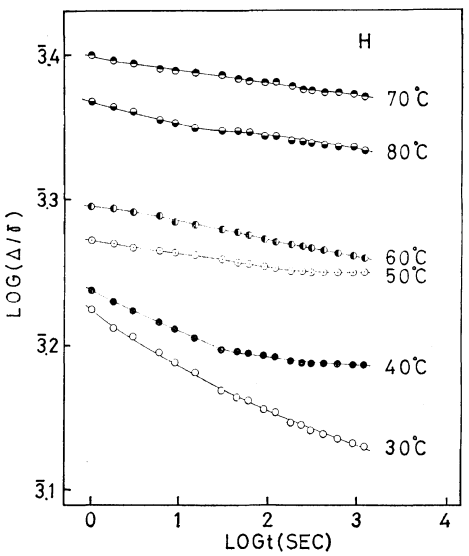

Figure 15. Strain—optical coefficient measured at various temperatures for sample H.

For reference, the stress-optical coefficient obtained for the samples A to H at 30°C is logarithmically plotted against time in Figure 17. The strain-optical coefficients for the samples A to F increase notably with time, while those for G and H are much less dependent on time.

The time—temperature superposition method was applied to the stress relaxation curves shown in Figures 7 to 10, as well as to the birefringence relaxation curves shown in Figures 12 to 15.

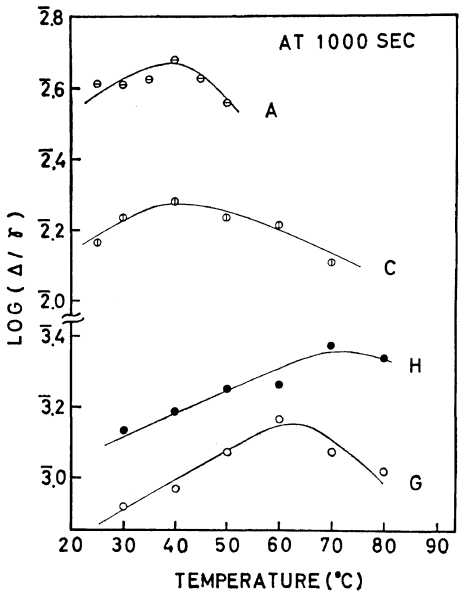

Figure 16. The variation of strain—optical coefficient with temperature for samples A, C, G, and H.

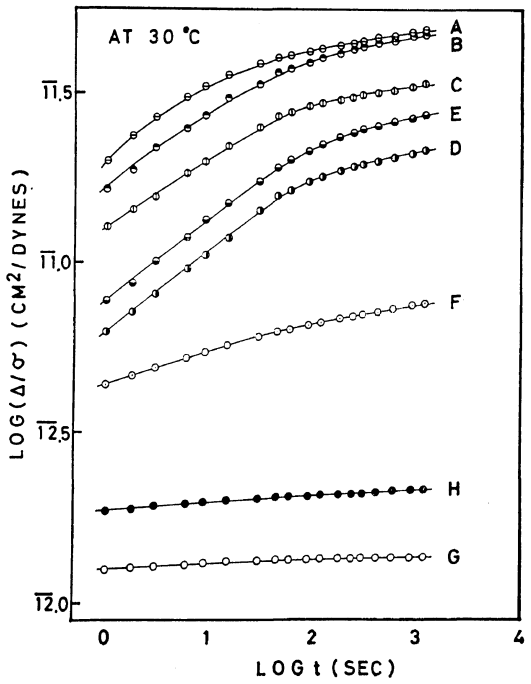

Figure 17. Stress—optical coefficient logarithmically plotted against time for all the samples.

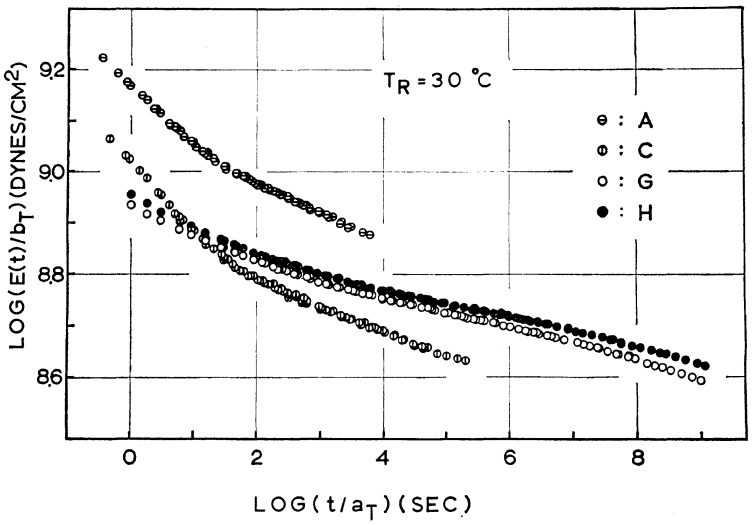

Figure 18. Master curves of relaxation modulus for samples A, C, G, and H.

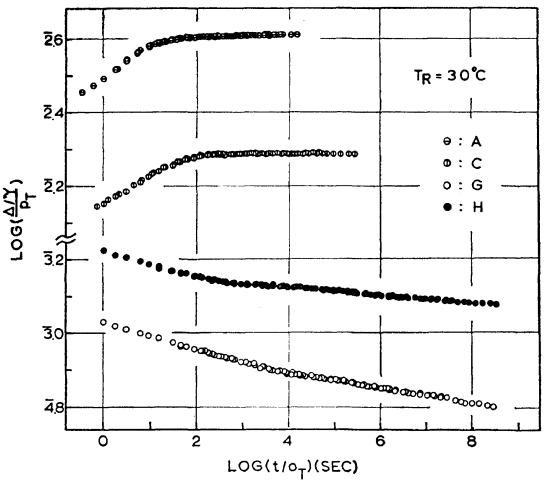

Figure 19. Master curves of strain—optical coefficient for samples A, C, G, and H.

In order to obtain smooth master curves, vertical shifts were required as well as horizontal shifts. Moreover, in the case of the samples A and C, the relaxation curves at the higher temperatures could not be superposed; the temperature limit of the superposition was equal to T_{max}. The $E(t)$ master curves for the four samples are

Table II. Activation energies for the samples A, C, G, and H

Sample	Activation energy, kcal/mol	
	Viscoelastic	Rheo-optical
A	28.4	28.4
C	34.4	34.4
G	55.6	55.6
H	54.4	54.4

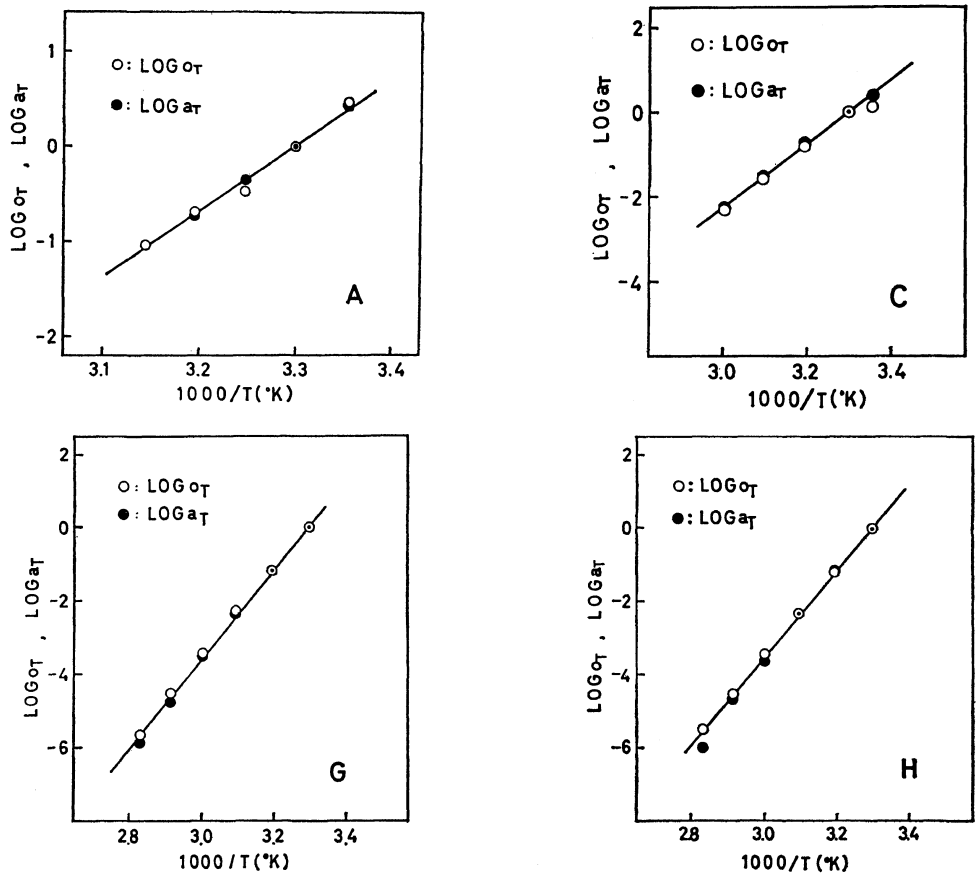

Figure 20. Viscoelastic and rheo-optical horizontal shift factors, a_T and o_T, plotted against $1/T$ for samples A, C, G, and H.

shown in Figure 18. The discrepancies between the samples becomes clearer if one compares the various relaxation spectra. This will be discussed later.

The corresponding master curves for the strain—optical coefficient Δ/γ of the same samples are shown in Figure 19.

The horizontal shift factors, designated by a_T for the viscoelastic factor and by o_T for the rheo-optical factor, when plotted logarithmically against the reciprocal of absolute temperature $1/T$, give the same straight line for a given sample, as is shown in Figure 20. This means that the viscoelastic and rheo-optical data are governed by the same activation energy. These activation energies, evaluated for the samples A, C, G, and H, are shown in Table II.

It is evident from this table that the activation energies for samples A and C are about 30 kcal/mol, while those for G and H are much higher. This difference in activation energy between the undrawn (or weakly drawn) films and the highly drawn films could have been anticipated from the fact that the time dependence of the birefringence was quite different. In other words, the rheo-optical properties of the highly drawn films, and thus the underlying deformation or orientation mechanisms, are quite different from those for the undrawn film. This will be discussed in more detail later.

The viscoelastic and rheo-optical vertical shift factors, b_T and p_T, are much smaller than a_T and o_T. The temperature dependence of b_T and p_T for samples A, C, G, and H is shown in Figure 21.

Relaxation Spectra and Deformation Mechanisms

From the master curves for $E(t)$ and Δ/γ shown in Figures 18 and 19, first-order approximations

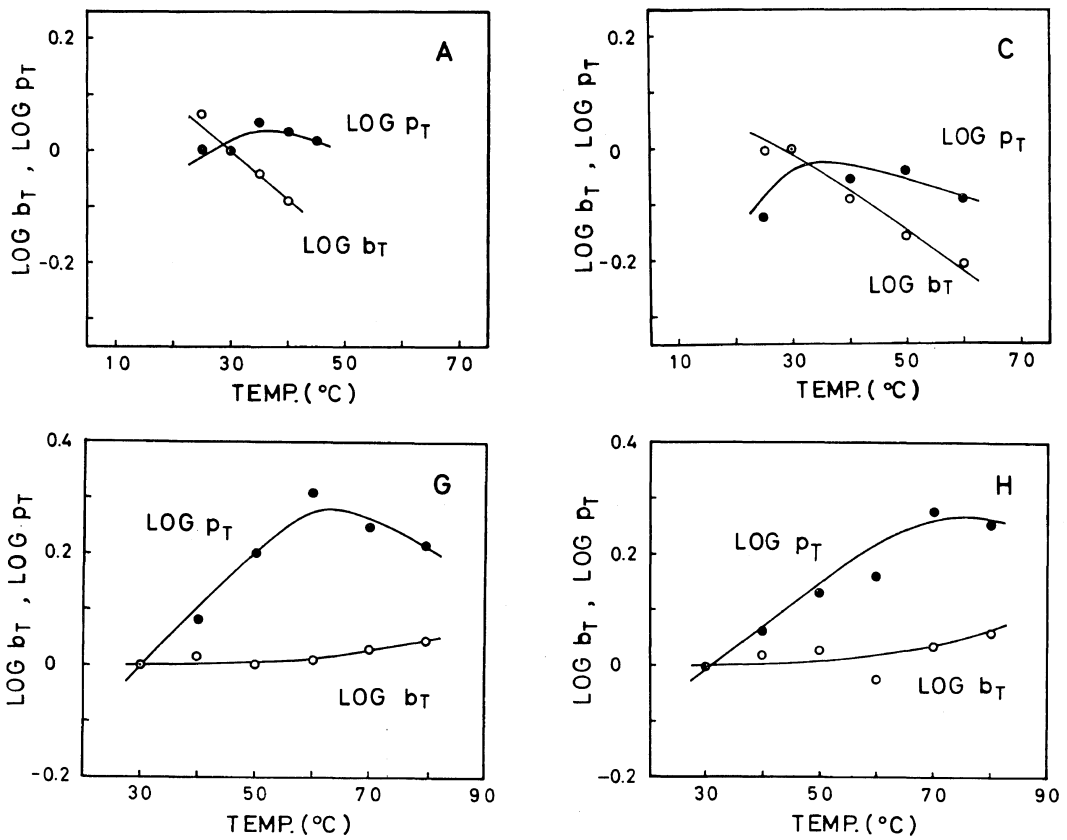

Figure 21. Viscoelastic and rheo-optical vertical shift factors, b_T and p_T, plotted against $1/T$ for samples A, C, G, and H.

for the viscoelastic and rheo-optical relaxation spectra were calculated by using the following relations:

$$H(\tau)=-\left[\frac{\partial E(t)}{\partial \ln t}\right]_{t=\tau} \quad (6)$$

$$B_0'-A_0'=\pm\left[\frac{\partial(\Delta/\gamma)}{\partial \ln t}\right]_{t=\tau} \quad (7)$$

The results are shown in Figure 22.

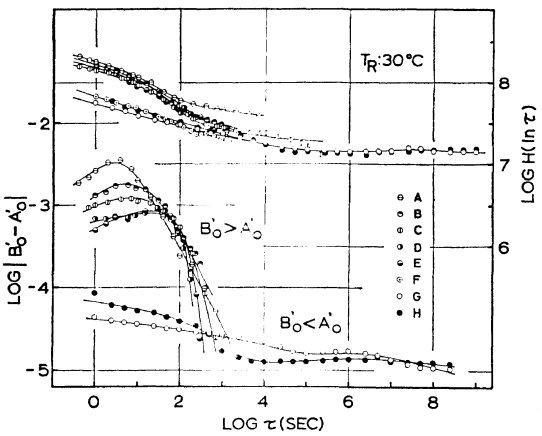

Figure 22. Viscoelastic and rheo-optical relaxation spectra for all the samples. The reference temperature is 30°C.

As is evident from this figure, the viscoelastic spectra for the samples A to F have a hump at the short-time end. Corresponding to this, the rheo-optical spectra have a peak in the same time range. But the hump and peak are missing from the spectra for the highly drawn samples G and H. Another notable difference in the rheo-optical spectra is in the relative magnitudes of A_0' and B_0'. In the case of samples A to F, A_0' is smaller than B_0', while in the case of G and H, A_0' is larger than B_0'.

According to our previous work, the peak in the rheo-optical spectrum at the short-time end corresponds to an increase in birefringence with time during a relaxation experiment and may be ascribed to the orientation of crystals in lamellae.[4] Generally speaking, the higher the degree of crystallinity, the higher the peak becomes.[11] However, the rheo-optical spectra shown in Figure 22 become lower and lower as the draw ratio, or degree of crystallinity, increases. This unusual behavior can be well explained by the following picture: suppose that the spherulites in the undrawn film are broken by drawing, the more so as the draw ratio increases; corresponding to this, the contribution of the crystalline orientation to the total birefringence becomes less and less. In the extreme case of the highly drawn films G and H, which have fiber structure, the spherulites are almost completely broken, and hence the contribution of the crystalline orientation disappears almost entirely. In other words, the decrease in birefringence with time observed for these highly oriented films should be due to a new, fourth relaxation mechanism. The activation energy for this type of process is about 55 kcal/mol, as is given in Table II, and is much greater than values of about 30 kcal/mol, which are characteristic of the crystalline orientation process.[5] The high activation energy found here is very similar to a value of 60 kcal/mol obtained for undrawn films of nylon 11 and 12 below 50°C.[3] In the case of the nylons, the birefringence also decreases with increasing time. Therefore, the higher activation energy of about 55 kcal/mol seems to be rather common for the primary dispersion of crystalline polymers. On the other hand, the lower activation energy (about 30 kcal/mol) can be said to be characteristic of the orientation of crystallites within spherulites of polyolefins.

When a spherulite in an undrawn or weakly drawn film of polyethylene deforms as a whole upon sudden stretching, various internal motions occur. Most lamellae are subjected mainly to stretching in the direction of their length, as well as to bending toward the direction of the stretching.

By such a process, the crystal *c*-axis orients perpendicular to the stretching direction. As time elapses, this orientation relaxes, and the *c*-axis orients to the direction of stretching, increasing the orientation function F_c, or the birefringence Δ, with increasing time. But the increase in F_c or Δ observed experimentally is larger than that expected from such a reorientation of the *c*-axis. Therefore, some other reversible process must be occurring simultaneously, such that the *c*-axis is oriented to the stretching direction even more. Some investigators consider that the

crystalline orientation occurs by slippage of crystal blocks past each other in the lamellae.[12,13] If such an irreversible change occurs, a film specimen used once for the relaxation measurement should change its spherulitic structure, and hence should manifest different birefringence behavior in subsequent measurements. However, if one carries out relaxation experiments only at small strains, this irreversible effect is not observed. Therefore, the idea of crystal slippage is not a reasonable explanation at small strains. The only reversible process that the authors can imagine is one in which the lamellae are locally twisted or untwisted, such that the *c*-axis is oriented to the stretching direction preferentially. Such a process can probably take place very easily in spherulites of polyolefins, but not in those of nylons. In nylons the lamellae probably have steady structure due to a high cohesive energy or strong hydrogen bonding between the molecules in the crystallites.[3]

In the case of the highly drawn films, amorphous molecular chains and crystallites which do not form spherulites are oriented in the stretching direction upon sudden stretching. As time elapses, this orientation relaxes, and the birefringence also simply relaxes. It cannot be confirmed that such a relaxation process occurs only in the crystalline region. Such a process would always be accompanied by the relaxation of amorphous chains.

Relaxation under Large Strains

Relaxation measurements following the application of several strain levels (3, 6, 9, and 12%) were also carried out with annealed films of low density polyethylene, Dow 544, at temperatures ranging from 15° to 90°C. In this strain range, the films were elongated uniformly, showing no necking, but the stress—strain behavior was nonlinear at strains of 6, 9, and 12%.

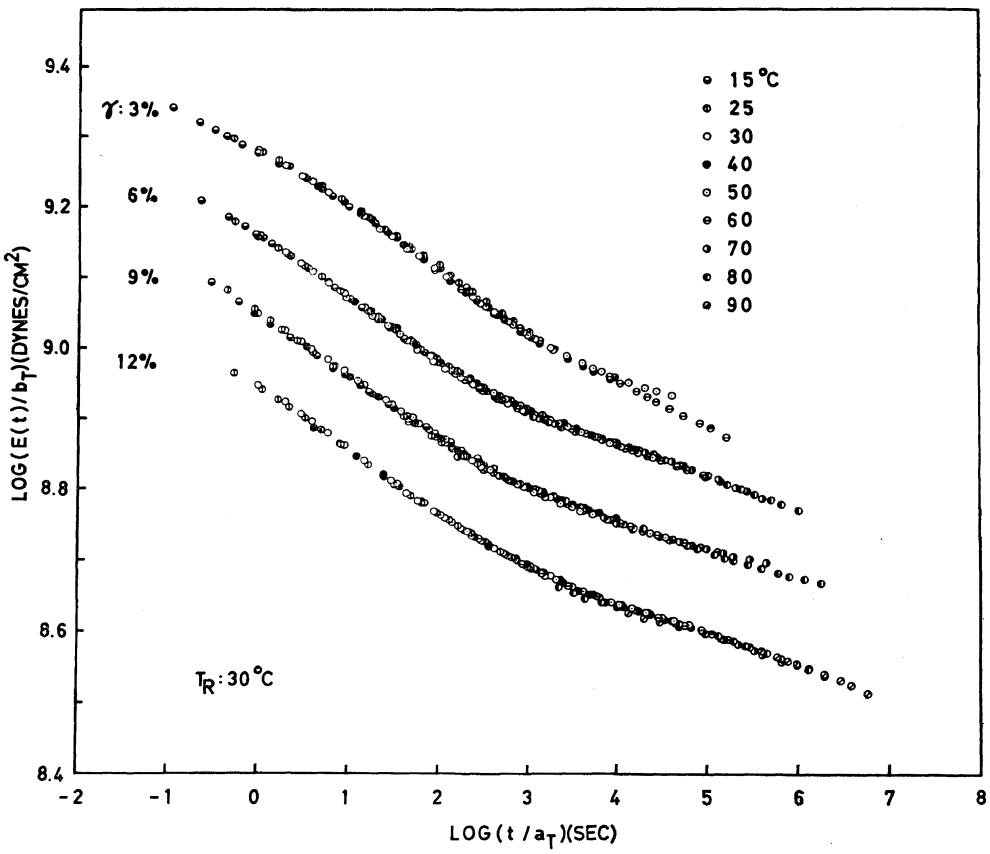

Figure 23. Master curves of the relaxation modulus measured at strain levels of 3, 6, 9, and 12%.

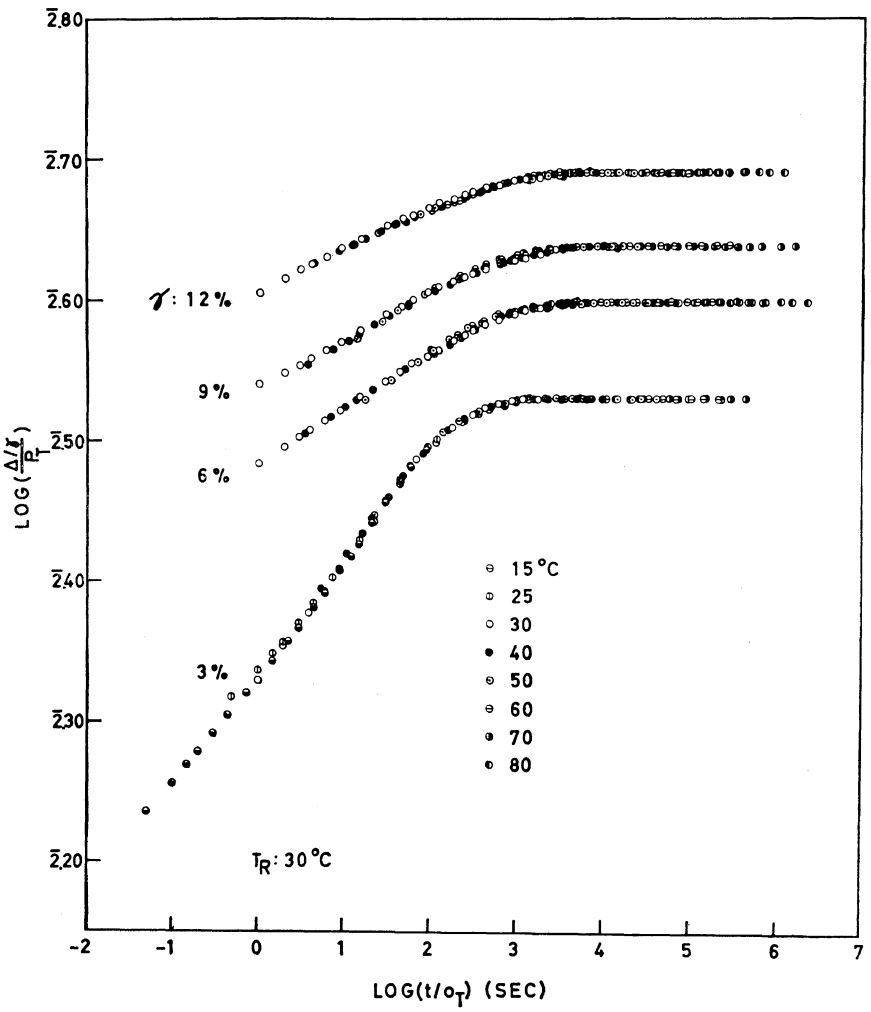

Figure 24. Master curves of the strain—optical coefficient measured at strain levels of 3, 6, 9, and 12%.

Master curves for the relaxation modulus $E(t)$ and the strain—optical coefficient Δ/γ, obtained by time—temperature superposition, are shown in Figures 23 and 24. As is evident from Figure 24, the increase in the strain—optical coefficient with time becomes small as the strain level increases. This is reflected more clearly in the height of the peak in the relaxation spectrum as shown in Figure 25. The higher the strain level, the lower the peak becomes. Such an effect of the strain level is very similar to the effect of drawing mentioned above. At higher levels of strain, spherulites in the sample film are broken to a greater extent, and this lessens the increase in birefringence caused by crystalline orientation. The breaking of the spherulites under large strains also seems to be one of prime factors in producing nonlinear viscoelastic behavior. We are now studying this effect further.

Activation energies for the relaxation processes were evaluated from the temperature dependences of the viscoelastic and the rheo-optical horizontal shift factors and are shown in Table III.

It is clear from this table that the activation energies from the viscoelastic and the rheo-optical data are almost the same, with a value of 29 kcal/mol and are independent of the strain levels. This value for the activation energy is

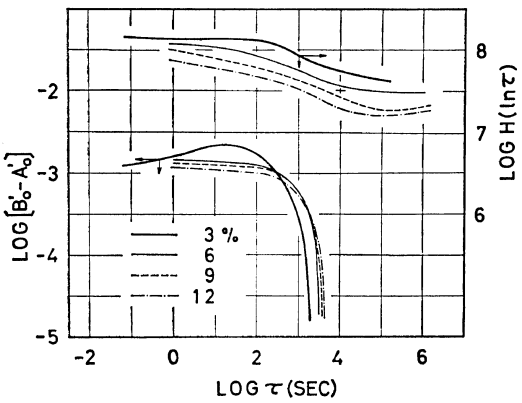

Figure 25. Viscoelastic and rheo-optical relaxation spectra determined at strain levels of 3, 6, 9, and 12%.

Table III. Viscoelastic and rheo-optical activation energies at different strain levels

Strain level, %	Activation energy, kcal/mol	
	Viscoelastic	Rheo-optical
3	29.3	29.3
6	27.1	30.1
9	27.6	29.2
12	30.6	26.9
Mean	28.7	28.9

consistent with those obtained previously for undrawn polyethylenes,[5] as well as with those obtained above for the undrawn and weakly drawn samples A and C.

Acknowledgment. This study was supported, in part, by a grant for scientific research (Kagaku Kenkyūhi Hojokin) from the Ministry of Education.

REFERENCES

1. Onogi Laboratory, "Rheo-Optical Studies of High Polymers, 1961-1970," 1971.
2. R. Yamada, C. Hayashi, and S. Onogi, *Zairyo*, **13**, 117 (1964).
3. S. Onogi, T. Asada, Y. Fukui, and I. Tachinaka, *Bull. Inst. Chem. Res., Kyoto Univ.*, **52**, 368 (1974).
4. S. Onogi, T. Asada, Y. Fukui, and T. Fujisawa, *Zairyo*, **15**, 390 (1966).
5. Y. Fukui, T. Sato, M. Ushirokawa, T. Asada, and S. Onogi, *J. Polym. Sci., Part A-2*, **8**, 1195 (1970).
6. R. Chiang and J. Flory, *J. Amer. Chem. Soc.*, **83**, 2857 (1961).
7. R. S. Stein, *J. Polym. Sci.*, **31**, 327, 335 (1950).
8. C. W. Bunn and R. deDaubeny, *Trans. Faraday Soc.*, **50**, 1173 (1954).
9. S. Hoshino, J. Powers, D. G. LeGrand, H. Kawai, and S. Stein, *J. Polym. Sci.*, **58**, 185 (1962).
10. S. Onogi, T. Asada, Y. Fukui, and T. Fujisawa, *J. Polym. Sci., Part A-2*, **5**, 1067 (1967).
11. R. S. Stein, S. Onogi, K. Sasaguri, and D. A. Keedy, *J. Appl. Phys.*, **34**, 80 (1963).
12. T. Oda, N. Sakaguchi, and H. Kawai, *J. Polym. Sci., Part C*, **15**, 223 (1966).
13. M. Takayanagi and T. Matsuo, *J. Macromol. Sci.*, **B1**, (3), 407 (1967).